Science and Technology Indonesia
e-ISSN:2580-4391 *p*-ISSN:2580-4405
Vol. 8, No. 3, July 2023

Research Paper

Activated Hydrochar Prepared from Longan Fruit (*Dimocarpus longan* Lour.) Peel via Hydrothermal Carbonization-NaOH Activation for Cationic Dyes Removal

Neza Rahayu Palapa[1], Alfan Wijaya[2], Nur Ahmad[2], Amri Amri[2], Risfidian Mohadi[2,3], Aldes Lesbani[2,3]*

[1]*Department of Chemistry, Faculty of Mathematics and Natural Sciences, Universitas Sriwijaya, Ogan Ilir, South Sumatra, 30862, Indonesia*
[2]*Research Centre of Inorganic Materials and Coordination Complexes, Graduate School of Universitas Sriwijaya, Palembang, South Sumatra, 30139, Indonesia*
[3]*Magister Program of Materials Science, Graduate School of Universitas Sriwijaya, Palembang, South Sumatra, 30139, Indonesia*
***Corresponding author**: aldeslesbani@pps.unsri.ac.id

Abstract
Hydrothermal carbonization is recognized as a method of processing biomass into carbon-rich products due to its energy-saving and environmental-friendly advantages. In this study, two types of hydrochar were prepared from Longan Fruit (*Dimocarpus longan* Lour.) Peel via hydrothermal carbonization at temperatures of 190°C and 250°C and activated using NaOH (HC-ACT 190 and HC-ACT 250) for removal of malachite green (MG) and rhodamine B (RhB) dyes. The maximum capacity for MG dye removal using HC-ACT 190 and HC-ACT 250 materials was 172.414 mg/g and 250 mg/g, while for RhB dye was 111.111 mg/g and 151.515 mg/g, respectively. The optimum pH was obtained at pH 6 for MG and pH 3 for RhB with adsorption equilibrium time occurring at 90 minutes. The kinetic study shows that the adsorption process follows pseudo-second-order kinetics, while the isotherm model was determined by the Langmuir isotherm model. Materials can be reused effectively for at least 3 cycles with an adsorption percentage of MG dye removal using HC-ACT 190 and HC-ACT 250 materials was 69.91% and 83.15% respectively, while for RhB dye was 35.79% and 55.6% respectively. The material is more selective on MG dye compared to RhB dye based on the selectivity test on the adsorption of the dye mixture.

Keywords
Longan Fruit Peel, Activated Hydrochar, Adsorption, Cationic Dye, Desorption, Regeneration

Received: 10 March 2023, Accepted: 27 June 2023
https://doi.org/10.26554/sti.2023.8.3.461-470

1. INTRODUCTION

Hydrothermal carbonization (HTC) converts biomass into carbon-rich products (hydrochar) and is usually carried out at a minimum temperature of 180°C to 300°C under autogenic pressure. This HTC method occurs under sub-critical hydrothermal reaction conditions and takes place under closed and high-pressure conditions, so the control is not as flexible as the pyrolysis method (Yang et al., 2023b; Czerwińska et al., 2023). The HTC process has several advantages, including being energy efficient as it can operate at relatively low temperatures, being able to process all types of wet biomass without going through an initial drying process, and the high surface area of the hydrocarbons produced (Ercan et al., 2023).

Biomasses converted to hydrocarbons via hydrothermal carbonization that have been reported include orange peels (Deepak et al., 2023), pomegranate peels (Khairy et al., 2022; Akkari et al., 2023), watermelon peel, banana peel, bay leaves (Yabalak and Elneccar, 2022), and pomelo peel (Zhu et al., 2023). Another biomass that can be converted into hydrocarbons through the hydrothermal carbonization process is longan fruit (*Dimocarpus longan* Lour.) peel. Longan fruit peel is a by-product that is often discarded and very rarely utilized so it is suitable to be converted into hydrochar to improve the physical ability and use value.

Hydrochar is widely used in various applications including catalysts (Baytar et al., 2023; Yabalak and Elneccar, 2022), supercapacitor (Xie et al., 2023), and adsorbents (Sanchez-Silva et al., 2022; Chen et al., 2023; Zhao et al., 2023). The process of increasing the porosity of hydrochar as an adsorbent by producing a very large surface area can be done through a chemical activation process using NaOH thus increasing the adsorption efficiency (Jais et al., 2021). Research conducted by da Silva Andrade et al. (2023), producing hydrochar from Pinus caribaea for adsorption of methylene blue and tartrazine yellow dyes resulted in a maximum capacity of 149 mg/g and 23.01 mg/g respectively. Jais et al. (2021) performed activation of hydrochar from sugarcane bagasse using NaOH with an increase in surface area to 22.552 m^2/g from 8.1 m^2/g in the initial material and the material was applied to the removal

of crystal violet dye which resulted in a maximum capacity of 47.97 mg/g.

In recent studies, hydrochar materials from biomass are widely used in dye removal due to the negative effects of these dyes. The discharge of artificial organic dyes widely used for dyeing in the textile industry into waters is becoming an urgent problem to be solved. These artificial organic dyes have high toxicity with a complex chemical structure that is very stable in water (Chowdhury et al., 2023; Wijaya et al., 2023). The negative effects of these organic dyes through water not only affect the photosynthesis, metabolism and growth processes of aquatic organisms, but also cause irreversible damage to humans when exposed to the body (Sun et al., 2023; Hakim et al., 2023). Based on the problems caused, there is a need for treatment to help remove these dye pollutants by utilizing biomass materials into products that have use value.

In this study, the preparation of hydrochar from longan fruit (*Dimocarpus longan* Lour.) peel was carried out by hydrothermal carbonization method and activation using NaOH. The material was investigated with several characterization data, including X-Ray Diffraction (XRD), Fourier Transform Infra-Red (FT-IR), Scanning Electron Microscope (SEM), and Brunauer-Emmett-Teller (BET) analysis. The material will be applied to remove malachite green (MG) and rhodamine B (RhB) dyes. The parameters used in this study include the effect of pH pzc, the effect of pH, adsorption contact time, the effect of initial concentration and temperature on the adsorption process, regeneration studies with desorption reagents, and adsorbent selectivity.

2. EXPERIMENTAL SECTION

2.1 Chemicals and Instrumentations

The longan fruit (*Dimocarpus longan* Lour.) peel in this study was sourced from Palembang, South Sumatra, Indonesia. The chemicals used in this study such as sodium hydroxide, sodium chloride and ethanol from EMSURE®, distilled water from Brataco, and hydrochloric acid from MallinckrodtAR®. Malachite green (MG) and rhodamine B (RhB) cationic dye powders were obtained from a textile factory. The materials were characterized using an X-Ray Rigaku Miniflex-600 Diffractometer, Shimadzu Prestige-21 FTIR Spectrophotometer, BET Surface Area Analyzer Micrometric ASAP Quantachrome, SEM Quanta-650 Oxford instrument, and absorbance measurement of solution using Biobase Spectrophotometer UV-Visible BKUV1800PC.

2.2 Preparation of Activated Hydrochar

Longan fruit (*Dimocarpus longan* Lour.) peel powder (LP) as much as 2.5 g was added to 50 mL of distilled water, then put into a 100 mL Hydrothermal Stainless-steel Autoclave tool and put into the oven at 190°C and 250°C for 10 hours, then allowed to stand at room temperature and washed with distilled water, then dried in an oven at 105°C for 24 hours. Hydrochar longan fruit peel that has been obtained is added to NaOH solution in a ratio of 1: 3 (hydrochar weight: NaOH percent) and put in a Stainless-steal Autoclave Hydrothermal tool then put in an oven at 110°C for 5 hours, then the temperature is increased to 250°C for 1 hour, then washed using hot distilled water until the pH is neutral, then dried in an oven at 105°C for 24 hours. Illustration of activated hydrochar preparation process is shown in Figure 1. Hydrochars with hydrothermal carbonization temperatures of 190 and 250 activated by NaOH (ACT-HC 190, and ACT-HC 250) were then characterized by XRD, FT-IR analysis, SEM, BET and tested on cationic dye removal.

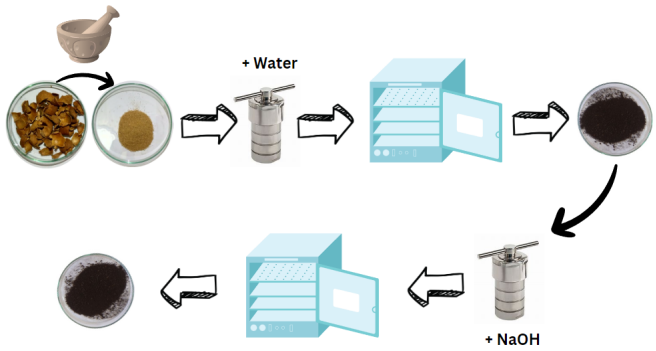

Figure 1. Illustration of Activated Hydrochar Preparation Process

2.3 pH points zero charges (pH_{pzc})

Determination of pH_{pzc} was carried out by adding 0.02 g of each adsorbent into 20 mL of NaCl solution with a concentration of 0.1 M which has been adjusted to pH with variations of pH 2, 3, 4, 5, 6, 7, 8, 9, 10, and 11. The mixture was stirred for 24 hours, then filtered and the filtrate was measured for final pH using a pH meter, then a graph was made of the relationship between initial pH and final pH.

2.4 Adsorption Study on MG and RhB Dyes

2.4.1 Variation of pH

A total of 0.02 g of adsorbent was added to 20 mL of green malachite dye solution and rhodamin-B with a concentration of 30 mg/L as much as 20 mL with variations in pH 2, 3, 4, 5, 6, 7, 8, 9, 10, and 11 and then stirred for 120 minutes, then the separation was carried out and the filtrate measured the absorbance value using a UV-Vis spectrophotometer at a wavelength of 617 nm for MG and 554 nm for RhB.

2.4.2 Variation of Contact Times

Adsorbent as much as 0.02 g was added to each dye solution with a concentration of 60 mg/L at the optimum pH that had been obtained. The adsorption process was stirred using a magnetic stirrer with a time variation of 10, 20, 30, 40, 50, 60, 70, 90, 100, 120, 150, 180, 210 and 240 minutes, then separation was carried out to separate the adsorbent with the dye and measured the absorbance value at the wavelength that had been obtained using a UV-Vis spectrophotometer.

© 2023 The Authors.

2.4.3 Variation of Temperature and Initial Concentration

0.02 g of adsorbent was added to 20 mL of dye solution with concentrations of (25, 50, 75, 100, and 125) mg/L which had been adjusted to the optimum pH value. Stirring was carried out using a magnetic stirrer during the optimum time obtained with temperature variations (30, 40, 50, 60, and 70) °C, then separation was carried out to separate the adsorbent with the dye. The filtrate obtained was measured for absorbance using a UV-Vis spectrophotometer.

2.4.4 Desorption and Regeneration Studies on Adsorbents

The desorption process is carried out by conducting an adsorption process first by adding MG and RhB dyes with a concentration of 60 mg/L, then adding 0.5 g of adsorbent, then the separation process is carried out by centrifuge and then dried. Desorption reagents used in the desorption process include hydrochloric acid with a concentration of 0.1 M, sodium hydroxide with a concentration of 0.1 M, ethanol and also use boiled water and distilled water, then each solvent as much as 20 mL is added to 0.02 g of adsorbents which has previously been used in the adsorption process, then stirring using a magnetic stirrer for 1 hour, then a separation process is carried out which aims to separate the adsorbent from the dye so that it can be reused in the regeneration process. The filtrate obtained was then measured for absorbance using a UV-Vis spectrophotometer.

The regeneration process was carried out by adding 0.02 g of adsorbent that had been desorbed into 20 mL of dye solution with a concentration of 60 mg/L, then stirred using a magnetic stirrer for 2 hours and separated by centrifuge. The filtrate obtained was then measured for absorbance using a UV-Vis spectrophotometer. The adsorbent was reused in the 2nd and 3rd desorption and adsorption processes.

2.4.5 Adsorbent Selectivity Test on MG and RhB Dyes Mixture

The adsorbent selectivity test on the MG and RhB dyes mixture was carried out by adding 0.02 g of adsorbent to 20 mL of MG and RhB dyes mixture with a concentration of 10 mg/L, then stirring with a variation of adsorption time of 15, 30, 60, 90, and 120 minutes, then filtering and the filtrate measured the wavelength at 500-700 nm using a UV-Vis spectrophotometer at each adsorption time.

3. RESULTS AND DISCUSSION

3.1 Characterizations

The XRD patterns of LP, ACT-HC 190, and ACT-HC 250 are shown in Figure 2(a). LP material that has been processed by hydrothermal carbonization-NaOH activation, there is a change in the diffraction peak which is getting wider. The broad peak at $2\theta = 24^\circ$ with reflected (002) carbon indicates the sample is carbonized due to the stacked aromatic layer structure. The broad peak is due to the presence of epoxy, carboxyl, and hydroxyl groups between the carbon atoms (Deepak et al., 2023). In addition, from the XRD results, there are also peaks of $2\theta = 15^\circ$ and 30°. These peaks are caused by the cellulose structure of the material (Baytar et al., 2023).

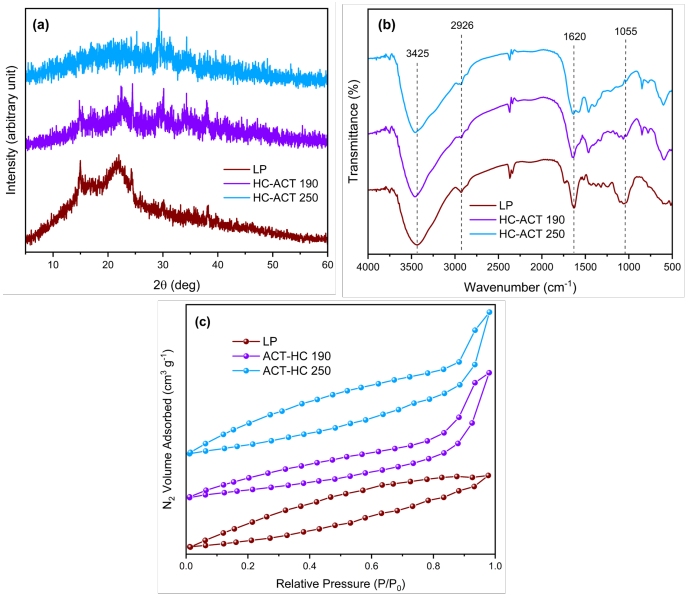

Figure 2. XRD Patterns (a), FT-IR Analysis (b), and N2 Adsorption-Desorption Properties (c) of LP, ACT-HC 190, and ACT-HC 250

The structure of the materials was determined by FT-IR spectroscopy in the wavenumber range of 4000-500 cm^{-1} and the results are given in Figure 2(b). The peak at a wave number around 3425 cm^{-1} indicates the presence of O-H which is due to the presence of water and alcohol. The wave number around 2926 cm^{-1} indicates the presence of C-H derived from alkyl groups. Vibrations at a wave number of about 1620 cm^{-1} indicate the presence of C-O derived from carbonyl compounds such as ketones, acids, aldehydes, and esters. Vibrations at wave number 1055 cm^{-1} indicate the presence of CO derived from ethers, alcohols, and phenols.

Table 1. Results of BET Analysis

Materials	Surface Area (m^2/g)	Pore Diameter (nm)	Pore Volume (cm^3/g)
LP	17.2	0.02	12.3
ACT-HC 190	10.2	0.04	13.4
ACT-HC 250	21.5	0.05	13.4

Figure 2(c) showed the N_2 Adsorption-Desorption Properties of materials. From Figure 2(c), the isotherm type of the material shows type IV isotherm and hysteresis phenomenon which classifies the material as having mesoporous structure with pore diameter <50 nm (Li et al., 2022). The results of BET analysis are shown in Table 1. HC-ACT 250 showed an increased surface area from the initial material so that the NaOH-activated hydrothermal carbonization process succeeded in im-

© 2023 The Authors.

proving the physical performance of the material. The surface area of HC-ACT 250 increased to 21.5 m^2/g from 17.2 m^2/g. The opposite happened to HC-ACT 190 which decreased the surface area to 10.2 m^2/g from 17.2 m^2/g. The cause of the decrease in surface area may be due to damage to the carbon structure or the formation of larger aggregates, thus reducing the overall surface area. The pore diameter and pore volume of the activated hydrocarbon material increased from the initial material. The pore diameter ranges from 0.02-0.05 nm which belongs to mesopores.

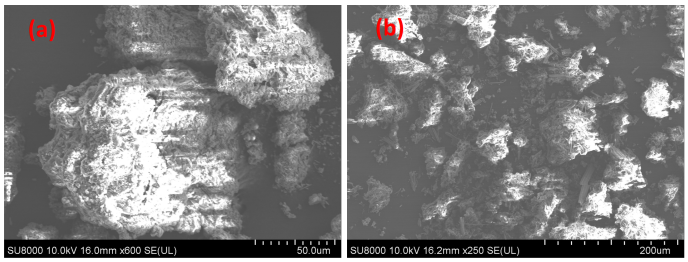

Figure 3. SEM Imagines of ACT-HC 190 (a) and ACT-HC 250 (b)

Figure 3 displays the SEM results used to characterize the surface morphology of the activated hydrochar produced. From Figure 3, it can be seen that HC-ACT 190 and HC-ACT 250 have a rough, fibrous and porous structure. In Figure 3, the surface morphology is agglomerated. The possible cause of the clumped hydrocarbon material is thought to be due to the polymerization process of the substrate dissolved in water to the surface of the hydrochar (Huang et al., 2021). The temperature and reaction time in the hydrothermal carbonization process can also affect agglomeration. Increased temperature and longer reaction times allow rearrangement and binding of particles, leading to agglomeration.

3.2 Effect of pH

The results of the pH_{pzc} material determination are shown in Figure 4. The pH_{pzc} of HC-ACT 190 and HC-ACT 250 were pH 9 and 10, respectively. Liu et al. (2023) reported that when adsorption optimum pH < pH_{pzc}, the surface of the material shows a positive charge, while when adsorption optimum pH > pH_{pzc}, shows a negative charge. In addition, Ahmad et al. (2023) reported that when the adsorption optimum pH = pH_{pzc} only physisorption occurs, while both physisorption and chemisorption occur at an optimum pH of adsorption optimum pH ≠ pH_{pzc}.

The effect of pH on MG and RhB dyes removal is shown in Figure 5. The MG dye removal process is more effective at pH 6 as shown in Figure 5(a). MG dyes in acidic conditions will be protonated due to excess H^+ ions and in basic conditions will be deprotonated due to excess OH^- ions. According to Eltaweil et al. (2020), the concentration of H^+ ions at acidic pH will increase the number of positive charges on the adsorbent surface, causing repulsion between the adsorbent and the

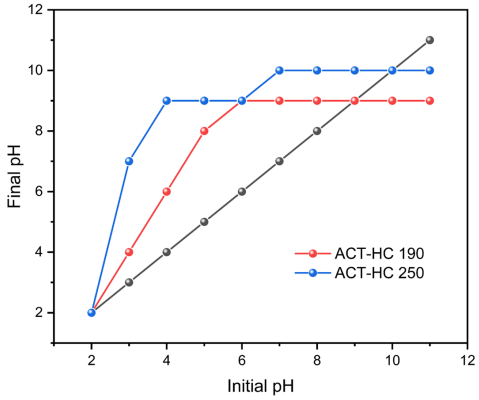

Figure 4. pH_{pzc} of the Materials

MG dye which is cationic which causes the adsorption process to be not optimal. Conversely, at neutral pH, the negative charge of OH^- ions on the adsorbent surface will increase, resulting in electrostatic attraction between the adsorbent and green malachite dye which causes the adsorption process to be optimal, while at pH above 6.9 the adsorption process is not optimal because the MG dye will experience deprotonation which causes changes in the dye structure. From Figure 5(b), the RhB dye removal process is more effective at pH 3. According to Adekola et al. (2019), RhB dye will form zwitter ions in water at pH above 3.7 which causes aggregation and the formation of larger molecules (dimers) so that the adsorption process is not optimal due to too large molecules that cannot enter the pores of the adsorbent, while at pH above 9 it will form zwitter ions and the surface of the adsorbent is negatively charged so that there is repulsion between the adsorbent and the dye so that the adsorption process is not optimal.

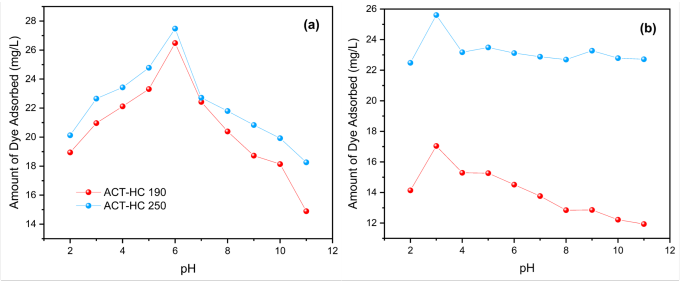

Figure 5. Effect of pH on MG and RhB Dyes Removal

In this study, the adsorption optimum pH < pHpzc in RhB dye removal, which indicates the adsorbent surface is positively charged, which allows the interaction of adsorbent and anionic dye electrostatically. In MG dye removal, pH < pHpzc, the composite surface showed a positive charge and there would be repulsion between the adsorbent and the cationic dye, but the material still showed a high removal rate of MG dye, which may be due to the chemical interactions that occurred. From the data of effect of pH experiments that have been carried out,

© 2023 The Authors.

Table 2. Adsorption Kinetic Models for MG and RhB Removal

Materials	Dyes	Qe_{exp} (mg/g)	Pseudo First Order			Pseudo Second Order		
			Qe_{calc} (mg/g)	k_1 (min^{-1})	R^2	Qe_{calc} (mg/g)	k_2 (g/mg min)	R^2
ACT-HC 190	MG	57.583	15.028	0.022	0.88	58.480	0.004	0.999
ACT-HC 250		57.698	7.055	0.033	0.884	58.140	0.016	0.999
ACT-HC 190	RhB	36.896	36.099	0.031	0.972	40.984	0.001	0.995
ACT-HC 250		53.219	33.713	0.034	0.984	56.180	0.002	0.999

it can be seen that the interaction occurs where the adsorption optimum pH ≠ pzc which indicates the occurrence of chemical and physical interactions.

3.3 Effect of Contact Times and Adsorption Kinetic Models

Effect of contact time on MG and RhB dyes removal are shown in Figure 6. Based on Figure 6, the MG and RhB dye removal process reached equilibrium after 90 minutes which was characterized by an insignificant increase in dye removal at times >90 minutes. The contact time effect data obtained was used to determine the adsorption kinetics model. There are two kinetic models used in this study, namely pseudo first-order (PFO) and pseudo second-order (PSO) adsorption kinetic models. Based on Table 2, the MG and RhB dye removal process is closer to the PSO adsorption kinetics model with a linear regression coefficient (R^2) value close to 1. This PSO model shows that the chemical adsorption process is most dominant in the adsorption process.

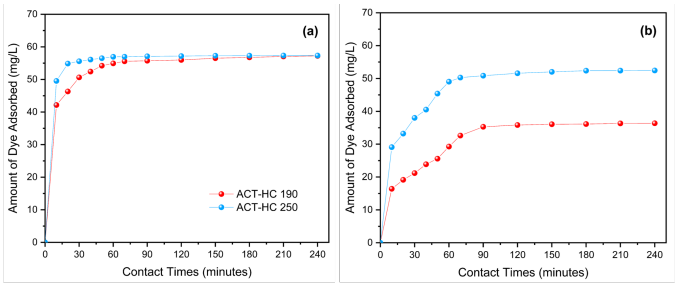

Figure 6. Effect of Contact Time on MG (a) and RhB (b) Dyes Removal

3.4 Adsorption Isotherm and Thermodynamic Models

Effect of initial concentration and temperature on MG and RhB dyes removal are shown in Figure 7. Based on Figure 7, the relationship between initial concentration and concentration to adsorption capacity is directly proportional, increasing initial concentration and temperature, the resulting adsorption capacity will also increase. The initial concentration and temperature effect data obtained were used for the determination of adsorption isotherms and thermodynamics. In this study, two adsorption isotherm models including Langmuir and Freundlich isotherms were used. Table 3 shows the comparison of Langmuir and Freundlich isotherm data. Table 3 shows a comparison of Langmuir and Freundlich isotherm data, where the MG and RhB dye removal process is more inclined to the Langmuir isotherm as indicated by a correlation value close to 1. The Langmuir isotherm assumes that the adsorption process occurs in a monolayer (chemisorption) (Amri et al., 2023).

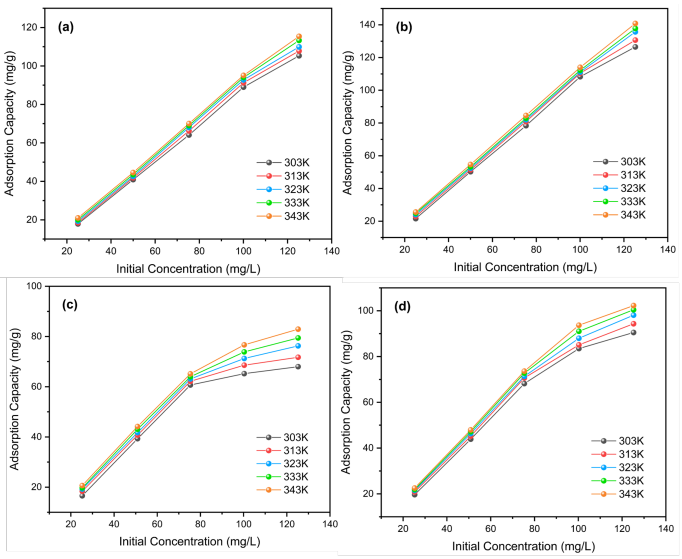

Figure 7. Effect of Initial Concentration and Temperature on Removal of MG Using HC-ACT 190 (b), and HC-ACT 250 (c), and RhB Using HC-ACT 190 (c), and HC-ACT 250 (d)

The maximum capacity of the MG and RhB dye removal process is listed in Table 3. The maximum capacity for MG dye removal using HC-ACT 190 and HC-ACT 250 materials was 172.414 mg/g and 250 mg/g, while for RhB dye was 111.111 mg/g and 151.515 mg/g, respectively. The resulting data shows that HC-ACT 250 has a greater maximum capacity for MG and RhB dye removal. The resulting maximum adsorption capacity value indicates how effective the material is in the dye removal process. The greater the maximum capacity produced, the more effective. MG dye removal was optimum at 40-50°C, while that of RhB dye was optimum at 30°C and tended to have no effect on adsorption capacity as temperature increased. At high temperatures, carbon materials can undergo structural changes, such as pore collapse, which leads to a reduction in surface area and thus decreases adsorption ability.

Table 4 shows a comparison of the maximum capacities for

© 2023 The Authors.

Table 3. Adsorption Isotherm Models for MG and RhB Dyes Removal

Dyes	Materials	Adsorption Isotherm	Adsorption Constant	Temperature (°C) 30	40	50	60	70
MG	HC-ACT 190	Langmuir	Qmax	107.527	129.870	172.414	120.482	125.000
			kL	0.030	0.031	0.030	0.047	0.056
			R^2	0.674	0.935	0.781	0.786	0.749
		Freundlich	n	0.617	0.664	0.740	0.670	0.671
			kF	1.221	2.090	3.712	3.679	4.981
			R^2	0.750	0.898	0.812	0.795	0.788
	HC-ACT 250	Langmuir	Qmax	212.766	250.000	84.746	78.125	84.034
			kL	0.023	0.026	0.069	0.087	0.114
			R^2	0.741	0.800	0.934	0.776	0.862
		Freundlich	n	0.784	0.843	0.559	0.539	0.645
			kF	3.932	6.409	2.774	3.477	9.504
			R^2	0.889	0.977	0.855	0.900	0.897
RhB	HC-ACT 190	Langmuir	Qmax	103.093	100.000	106.383	109.890	111.111
			kL	0.040	0.056	0.060	0.066	0.080
			R^2	0.980	0.984	0.865	0.868	0.901
		Freundlich	n	1.724	1.817	1.783	1.800	1.845
			kF	7.905	9.786	10.399	11.452	13.152
			R^2	0.619	0.699	0.713	0.716	0.746
	HC-ACT 250	Langmuir	Qmax	151.515	138.889	142.857	135.135	128.205
			kL	0.050	0.076	0.092	0.126	0.183
			R^2	0.959	0.999	0.973	0.976	0.982
		Freundlich	n	1.612	1.939	1.948	2.372	2.884
			kF	12.092	18.038	20.403	27.606	35.124
			R^2	0.961	0.583	0.637	0.546	0.942

MG and RhB dye removal that have been reported. From the Table 4, it shows that the HC-ACT 190 and HC-ACT 250 materials have greater adsorption capacities so that it can be assumed that the materials in this study can be used as effective materials in the removal of cationic dyes, especially MG and RhB.

The thermodynamic parameters are shown in Table 5. Based on Table 5, it can be seen that the overall ΔG value is negative indicating the adsorption process takes place spontaneously and the ΔH value is positive indicating the endothermic properties during the adsorption process. The ΔS value indicates the degree of irregularity, where the ΔS value of HC-ACT 250 is greater than HC-ACT 250.

3.5 Desorption and Regeneration

The desorption process aims to remove the dye that has been adsorbed on the material so that the material can be reused or regenerated. The desorption process in this study uses several organic and inorganic reagents to see the effectiveness of the reagents in desorbing the dye on the material. Desorption of MG and RhB dyes on materials using several reagents are shown in Figure 8. From the Figure 8, the effective reagent to desorb MG in HC-ACT 190 and 250 materials is NaOH, the same for RhB in HC-ACT 190 material is NaOH, while in HC-ACT 250 material, ethanol is more effective in desorbing RhB dye. NaOH reagent was able to desorb MG on HC-ACT 190 and 250 materials by 7.12% and 5.12% respectively, while on RhB dye for HC-ACT 190 material by 16.01%. RhB dye was desorbed by 15.59% using ethanol reagent on HC-ACT 250. NaOH reagent is more effectively used as a desorption reagent assumed due to the involvement of acid-base reactions in the desorption process, while ethanol reagent is more effective due to the influence of like dissolved like between adsorbate and solvents that are polar in the desorption process.

The material regeneration process is carried out to see the ability of materials that can be used repeatedly. In recent studies, materials that have high stability in the regeneration process are a unique advantage. Regeneration ability of materials on

© 2023 The Authors.

Table 4. Comparison of Adsorption Ability on the MG and RhB Dyes Removal by Several Adsorbents

Dyes	Adsorbents	Adsorption Capacity (mg/g)	References
MG	Sulfur-doped Biochar Derived from Tapioca Peel Waste	30.18	(Vigneshwaran et al., 2021)
	Chinese Fan-Palm Biochar (Livistona chinensis)	21.4	(Giri et al., 2022)
	Mn_3O_4 Nanoparticles using Costus woodsonii Flowers Extract	162	(Van Tran et al., 2022)
	Polyaniline Facilitated Cobalt Phosphate Nanocomposite	185.62	(Ben et al., 2023)
	Demethylated Lignin-based Micro-particle	168.24	(Du et al., 2023)
	HC-ACT 190	172.414	This study
	HC-ACT 250	250	This study
RhB	Sulfur-doped Biochar Derived from Tapioca Peel Waste	33.10	(Vigneshwaran et al., 2021)
	NiZnAl-LDHs	97.09	(Nazir et al., 2022)
	Magnetic K_2CO_3-activated Carbon Produced from Bamboo Shoot	53.931	(Wu et al., 2023)
	Manganese Titanium Oxide Composite Biochar	19.061	(Yang et al., 2023a)
	Fe-modified Hydrochar derived from wheat straw	80	(Kohzadi et al., 2023)
	HC-ACT 190	111.111	This study
	HC-ACT 250	151.515	This study

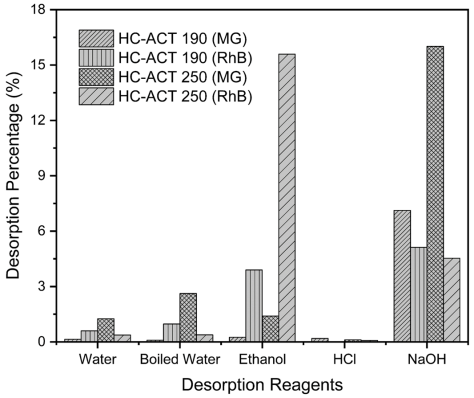

Figure 8. Desorption of MG and RhB Dyes on Materials Using Several Reagents

MG and RhB dyes removal are shown in Figure 9. Based on the material regeneration ability data in Figure 9, it shows that HC-ACT 190 and HC-ACT 250 can be used repeatedly for 3 cycles in the MG and RhB dye removal process. The adsorption percentage in the third cycle for MG dye removal using HC-ACT 190 and HC-ACT 250 materials was 69.91% and 83.15% respectively, while for RhB dye was 35.79% and 55.6% respectively. At more than 3 cycles, the material experienced a significant decrease in adsorption ability so only 3 cycles are shown in this study.

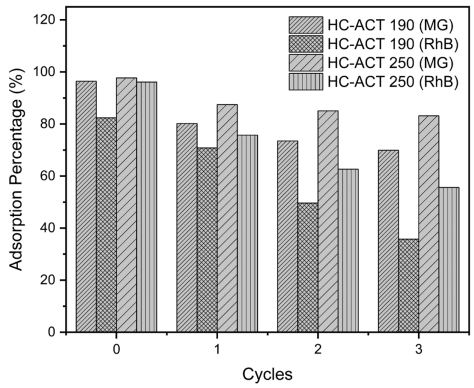

Figure 9. Regeneration Ability of Materials on MG and RhB Dyes Removal

3.6 Materials Selectivity Test

The material selectivity test aims to see which dye is more selective for the material. This test can be determined through a wavelength scan on the adsorption of a dye mixture within a certain time range. The wavelength scan of the adsorption of a mixture of MG and RhB dyes at several contact times is shown in Figure 10. Based on the data in Figure 10, it shows that MG dyes are more selective than RhB dyes as evidenced by

© 2023 The Authors.

Table 5. Thermodynamic Parameters

Dyes	Materials	Concentration (mg/L)	T (K)	Qe (mg/g)	ΔH (kJ/mol)	ΔS(J/mol. K)	ΔG (kJ/mol)
MG	HC-ACT 190	125.207	303	105.290	17.331	0.071	-4.082
			313	107.801			-4.788
			323	109.915			-5.495
			333	113.253			-6.202
			343	115.351			-6.908
	HC-ACT 250		303	107.541	27.347	0.105	-4.447
			313	111.078			-5.496
			323	115.333			-6.545
			333	117.132			-7.595
			343	119.735			-8.644
RhB	HC-ACT 190	125.236	303	67.989	10.879	0.037	-0.420
			313	71.723			-0.793
			323	76.266			-1.166
			333	79.415			-1.538
			343	82.924			-1.911
	HC-ACT 250		303	90.517	11.748	0.047	-2.443
			313	94.318			-2.911
			323	98.075			-3.379
			333	100.436			-3.848
			343	102.281			-4.316

a significant decrease in absorbance at more than 0.25 hours. Absorbance is directly proportional to concentration, a significant decrease in the absorbance of MG dye compared to RhB indicates that there is little concentration of MG remaining in the mixture. This shows that the MG dye is more adsorbed on the material compared to the RhB dye. The cause of the material is not more selective to RhB which may occur because the molecular structure is larger than MG so that it affects the adsorption process.

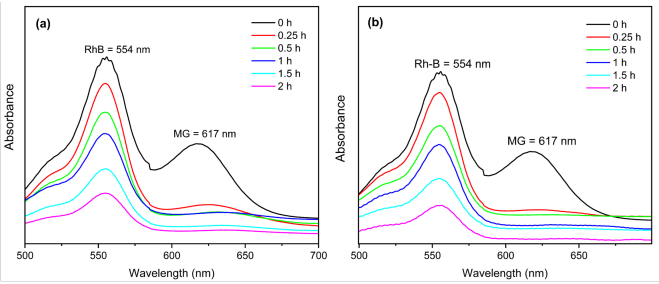

Figure 10. Wavelength Scan on Adsorption of MG and RhB Dyes Mixture Using HC-ACT 190 (a) and HC-ACT 250 (b) at Several Contact Times

3.7 Characterization of Material After Dye Adsorption

Characterization of the material after being adsorbed by the dye aims to see the changes that occur in the material. In this study, the characterization used is XRD. Figure 11 shows the XRD patterns of HC-ACT 250 before and after adsorption of MG and RhB dyes. Based on the XRD data in Figure 11, it can be seen that in the material that has been adsorbed on MG and RhB, the diffraction peaks at around 20° have wider peak changes, while at a diffraction angle of around 30° there are increasingly sharp peak changes. The changes in the diffraction peaks indicate the occurrence of certain molecular interactions between the dye and the material. The interactions

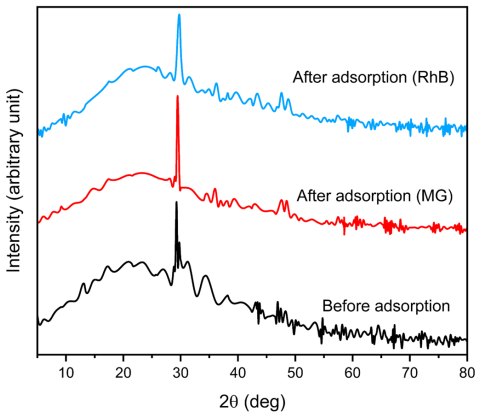

Figure 11. XRD Patterns of HC-ACT 250 (Before and After Adsorption of MG and RhB Dyes)

© 2023 The Authors.

that occur can be in the form of hydrogen bonds or other intermolecular interactions between the dye and the material during the adsorption process which can result in shifts or changes in the diffraction peaks due to changes in the structure of the material.

4. CONCLUSION

Activated hydrochar has been successfully prepared to removal of MG and RhB dyes with high adsorption capacity. The optimum pH was obtained at pH 6 for MG and pH 3 for RhB with adsorption equilibrium time occurring at 90 minutes. The kinetic study shows that the adsorption process follows PSO kinetics model, while the isotherm model was determined by the Langmuir isotherm model. The material can be reused effectively for at least 3 cycles. This material is more selective on MG dye compared to RhB dye.

5. ACKNOWLEDGMENT

The authors thank to Research Centre of Inorganic Materials and Coordination Complexes, Magister Program of Materials Science, Graduate School of Universitas Sriwijaya, Universitas Sriwijaya for support and instrumental analysis.

REFERENCES

Adekola, F. A., S. B. Ayodele, and A. A. Inyinbor (2019). Efficient Rhodamine B Removal Using Acidand Alkaline-activated *Musa paradisiaca* Biochar. *Polish Journal of Environmental Studies*, **28**(5); 3063–3070

Ahmad, N., F. S. Arsyad, I. Royani, P. M. S. B. N. Siregar, T. Taher, and A. Lesbani (2023). High Regeneration of ZnAl/NiAl-Magnetite Humic Acid for Adsorption of Congo Red from Aqueous Solution. *Inorganic Chemistry Communications*, **150**; 110517

Akkari, I., L. Spessato, Z. Graba, N. Bezzi, and M. M. Kaci (2023). A Sustainably Produced Hydrochar from Pomegranate Peels for the Purification of Textile Contaminants in an Aqueous Medium. *Sustainable Chemistry and Pharmacy*, **31**; 100924

Amri, A., A. Lesbani, and R. Mohadi (2023). Malachite Green Dye Adsorption from Aqueous Solution Using a Ni/Al Layered Double Hydroxide-Graphene Oxide Composite Material. *Science and Technology Indonesia*, **8**(2); 280–287

Baytar, O., Ö. Şahin, and A. Ekinci (2023). Effect of Environmentally Friendly and Efficient Metal-free Hydrochars as Catalysts on Sodium Borohydride Hydrolysis. *Fuel*, **346**; 128308

Ben, S. K., S. Gupta, K. K. Raj, and V. Chandra (2023). Adsorption of Malachite Green from Polyaniline Facilitated Cobalt Phosphate Nanocomposite from Aqueous Solution. *Chemical Physics Letters*, **820**; 140469

Chen, Y., S.-A. Huang, K. Yu, J.-Z. Guo, Y.-X. Wang, and B. Li (2023). Adsorption of Lead Ions and Methylene Blue on Acrylate-modified Hydrochars. *Bioresource Technology*, **379**; 129067

Chowdhury, M. F., C.-M. Kim, and A. Jang (2023). High-efficient and Rapid Removal of Anionic and Cationic Dyes Using a Facile Synthesized Sole Adsorbent NiAlFe-layered Triple Hydroxide (LTH). *Chemosphere*, **332**; 138878

Czerwińska, K., A. Marszałek, E. Kudlek, M. Śliz, M. Dudziak, and M. Wilk (2023). The Treatment of Post-processing Liquid from the Hydrothermal Carbonization of Sewage Sludge. *Science of The Total Environment*, **885**; 163858

da Silva Andrade, J. G., C. E. Porto, W. M. Moreira, V. R. Batistela, and M. H. N. O. Scaliante (2023). Production of Hydrochars from *Pinus caribaea* for Biosorption of Methylene Blue and Tartrazine Yellow Dyes. *Cleaner Chemical Engineering*, **5**; 100092

Deepak, K., S. Mohan, P. Dinesha, and R. Balasubramanian (2023). CO_2 Uptake by Activated Hydrochar Derived from Orange Peel (*Citrus reticulata*): Influence of Carbonization Temperature. *Journal of Environmental Management*, **342**; 118350

Du, B., L. Chai, Y. Wang, X. Wang, X. Chen, J. Zhou, and R.-C. Sun (2023). Fabrication of Demethylated Lignin-based Micro-particle for Efficient Adsorption of Malachite Green from Aqueous Solution. *Journal of Molecular Liquids*, **382**; 121935

Eltaweil, A., H. A. Mohamed, E. M. Abd El-Monaem, and G. El-Subruiti (2020). Mesoporous Magnetic Biochar Composite for Enhanced Adsorption of Malachite Green Dye: Characterization, Adsorption Kinetics, Thermodynamics and Isotherms. *Advanced Powder Technology*, **31**(3); 1253–1263

Ercan, B., K. Alper, S. Ucar, and S. Karagoz (2023). Comparative Studies of Hydrochars and Biochars Produced from Lignocellulosic Biomass via Hydrothermal Carbonization, Torrefaction and Pyrolysis. *Journal of the Energy Institute*; 101298

Giri, B. S., R. K. Sonwani, S. Varjani, D. Chaurasia, T. Varadavenkatesan, P. Chaturvedi, S. Yadav, V. Katiyar, R. S. Singh, and A. Pandey (2022). Highly Efficient Bio-adsorption of Malachite Green Using Chinese Fan-Palm Biochar (*Livistona chinensis*). *Chemosphere*, **287**; 132282

Hakim, Y. M., R. Vinsiah, and S. Fajri (2023). High Efficient of Ca/Al-Graphite for Removal of Direct Orange. *Indonesian Journal of Material Research*, **1**(1); 15–22

Huang, Z., L. Shi, Y. Muhammad, and L. Li (2021). Effect of Ionic Liquid Assisted Hydrothermal Carbonization on the Properties and Gasification Reactivity of Hydrochar Derived from Eucalyptus. *Journal of Colloid and Interface Science*, **586**; 423–432

Jais, F. M., C. Y. Chee, Z. Ismail, and S. Ibrahim (2021). Experimental Design via NaOH Activation Process and Statistical Analysis for Activated Sugarcane Bagasse Hydrochar for Removal of Dye and Antibiotic. *Journal of Environmental Chemical Engineering*, **9**(1); 104829

Khairy, G. M., A. M. Hesham, H. E. S. Jahin, S. A. El-Korashy, and Y. M. Awad (2022). Green Synthesis of a Novel Eco-friendly Hydrochar from Pomegranate Peels Loaded with

© 2023 The Authors.

Iron Nanoparticles for the Removal of Copper Ions and Methylene Blue from Aqueous Solutions. *Journal of Molecular Liquids*, **368**; 120722

Kohzadi, S., N. Marzban, J. A. Libra, M. Bundschuh, and A. Maleki (2023). Removal of RhB from Water by Fe-modified Hydrochar and Biochar–An Experimental Evaluation Supported by Genetic Programming. *Journal of Molecular Liquids*, **369**; 120971

Li, Y., M. Wu, J. Wu, Y. Wang, Z. Zheng, and Z. Jiang (2022). Mechanistic Insight and Rapid Co-adsorption of Nitrogen Pollution from Micro-polluted Water Over MgAl-layered Double Hydroxide Composite Based on Zeolite. *Separation and Purification Technology*, **297**; 121484

Liu, Y., D. Zhong, Y. Xu, H. Chang, L. Dong, Z. Han, J. Li, and N. Zhong (2023). Adsorption of Phosphate in Water by La/Al Bimetallic-organic Frameworks-chitosan Composite with Wide Adaptable pH Range. *Journal of Environmental Chemical Engineering*; 110309

Nazir, M. A., T. Najam, S. Jabeen, M. A. Wattoo, M. S. Bashir, S. S. A. Shah, and A. ur Rehman (2022). Facile Synthesis of Tri-metallic Layered Double Hydroxides (NiZnAl-LDHs): Adsorption of Rhodamine-B and Methyl Orange from Water. *Inorganic Chemistry Communications*, **145**; 110008

Sanchez-Silva, J. M., V. H. Collins-Martínez, E. Padilla-Ortega, A. Aguilar-Aguilar, G. J. Labrada-Delgado, O. Gonzalez-Ortega, G. Palestino-Escobedo, and R. Ocampo-Pérez (2022). Characterization and Transformation of Nanche Stone (*Byrsonima crassifolia*) in an Activated Hydrochar with High Adsorption Capacity towards Metformin in Aqueous Solution. *Chemical Engineering Research and Design*, **183**; 580–594

Sun, S., E. Yu, R. Hu, Y. Li, and Z. Wei (2023). Synthesis and Study of Poly (Phthalic Anhydride-β-cyclodextrin) for the Efficient Adsorption of Cationic Dyes from Industrial Wastewater. *Chemical Engineering Research and Design*, **194**; 768–778

Van Tran, T., D. T. C. Nguyen, P. S. Kumar, A. T. M. Din, A. S. Qazaq, and D.-V. N. Vo (2022). Green Synthesis of Mn_3O_4 Nanoparticles Using *Costus woodsonii* Flowers Extract for Effective Removal of Malachite Green Dye. *Environmental Research*, **214**; 113925

Vigneshwaran, S., P. Sirajudheen, P. Karthikeyan, and S. Meenakshi (2021). Fabrication of Sulfur-doped Biochar Derived from Tapioca Peel Waste with Superior Adsorption Performance for the Removal of Malachite Green and Rhodamine B Dyes. *Surfaces and Interfaces*, **23**; 100920

Wijaya, A., P. M. S. B. N. Siregar, A. F. Badri, N. R. Palapa, A. Amri, N. Ahmad, and A. Lesbani (2023). Modified Layered Double Hydroxide Mg/M3+ (M3+= Al and Cr) Using Metal Oxide (Cu) as Adsorbent for Methyl Orange and Methyl Red Dyes. *Periodica Polytechnica Chemical Engineering*, **67**(2); 173–184

Wu, W., C. Wu, G. Zhang, J. Liu, Y. Li, and G. Li (2023). Synthesis and Characterization of Magnetic K_2CO_3-activated Carbon Produced from Bamboo Shoot for the Adsorption of Rhodamine B and CO_2 Capture. *Fuel*, **332**; 126107

Xie, D., J. Huang, Z. Wang, W. Hu, C. Liu, D. Wang, X. Li, and Y. Qiao (2023). Activated Carbon Derived from Hydrochar of Food Waste for Supercapacitor: Effect of Components on Electrochemical Performance. *Fuel Processing Technology*, **244**; 107691

Yabalak, E. and F. Elneccar (2022). Evaluation of Watermelon Peel, Banana Peel and Bay Leaves Hydrochars as Green Catalysts in the Degradation of Malachite Green by Thermally Activated Persulfate Oxidation Method. *Journal of Environmental Management*, **304**; 114311

Yang, J., Q. Wei, D. Li, J. Yu, and Z. Cai (2023a). Study on Adsorption Performance of Manganese Titanium Oxide Composite Biochar for Removal of Rhodamine B. *Journal of the Indian Chemical Society*, **100**(4); 100958

Yang, J., Z. Zhang, J. Wang, X. Zhao, Y. Zhao, J. Qian, and T. Wang (2023b). Pyrolysis and Hydrothermal Carbonization of Biowaste: A Comparative Review on the Conversion Pathways and Potential Applications of Char Product. *Sustainable Chemistry and Pharmacy*, **33**; 101106

Zhao, F., L. Tang, H. Jiang, Y. Mao, W. Song, and H. Chen (2023). Prediction of Heavy Metals Adsorption by Hydrochars and Identification of Critical Factors Using Machine Learning Algorithms. *Bioresource Technology*, **383**; 129223

Zhu, F., Z. Wang, J. Huang, W. Hu, D. Xie, and Y. Qiao (2023). Efficient Adsorption of Ammonia on Activated Carbon from Hydrochar of Pomelo Peel at Room Temperature: Role of Chemical Components in Feedstock. *Journal of Cleaner Production*, **406**; 137076

© 2023 The Authors.